Supplementary Information for

Programmable Chiral States in Flocks of Active Magnetic Rollers

Koohee Han*[a] and Alexey Snezhko[a]

[a] *Materials Science Division, Argonne National Laboratory, Lemont, IL 60439, USA.*

*Corresponding author. E-mail: hank@anl.gov

Legends for Movies S1 to S6

Movie S1. Magnetic field-driven chirality switching in a vortex of magnetic rollers. The vortex alternatively swithces its chirality between right- and left-handedness during 10 consecutive cycles. The chirality switching is driven by the introduction of a π phase shift with respect to the preceding magnetic field signal. Each cycle is 2.5 sec. f = 40 Hz, H_0 = 35 Gauss. Real-time playback.

Movie S2. Magnetic field-driven phase transition in a collection of magnetic rollers. The magnetic rollers intially exhibit the gas phase at f = 20 Hz, evolve into the flocking phase at f = 30 Hz, and finally develop the vortex phase at f = 40 Hz. Each cycle is 5 sec. H_0 = 35 Gauss. Real-time playback.

Movie S3. Reversal in the moving direction of a single roller. Initially, the roller keeps moving along the droplet edge clockwise with the continuous application of the sinusoidal magnetic field. The roller ceases its motion upon removal of the field. The re-application of the field with a π phase shift (i.e., inverted sinusoidal field) reverses the rolling direction of the roller and thus its moving direction along the drople edge from clockwise to counterclockwise. f = 40 Hz, H_0 = 35 Gauss. Real-time playback.

Movie S4. Programmable chirality switching 1. The chiral states of the two isolated vorticies with opposite chiralities are under control by the pre-programmed magnetic signals shown in Fig. 3e during 6 consecutive cycles: The vorticies simultaneously switch their chirality upon the introduction of a π phase shift to the preceding magnetic signal (e.g., Cycle 1 $\rightarrow$ 2) while they maintain their chirality in the absence of the phase shift (e.g., Cycle 3 $\rightarrow$ 4). Each cycle is 5 sec. f = 40 Hz, H_0 = 35 Gauss. Real-time playback.

Movie S5. Programmable chirality switching 2. The magnetic signals shown in Fig. 3e are used again to control the chiral states of the two isolated vorticies with same chiralities in the same programmed sequnece implemented in Movie S4. The only difference between Movie S4 and S5 is the initial chiral states in the two vorticies. Despite the different initial chiral states, the vortices display the same order of chirality switching in Movie S5. Each cycle is 5 sec. f = 40 Hz, H_0 = 35 Gauss. Real-time playback.

Movie S6. Self-assembled remotely switchable micro-pump device. Initially, the magnetic rollers circulate on the pump device in a clockwise fashion witn the application of the sinusoidal magnetic field. The rollers carry the surrounding fluid in the same direction of their motion where the fluid transport is visualized by the addition of a water-miscible dye. Upon removal of the field, the rollers cease their motion and the fluid transport is halted. The re-application of the field with a π phase shift (i.e., inverted sinusoidal field) allows the rollers to transport the fluid in the opposite direction as confirmed by the dye flow. f = 50 Hz, H_0 = 35 Gauss. Real-time playback.

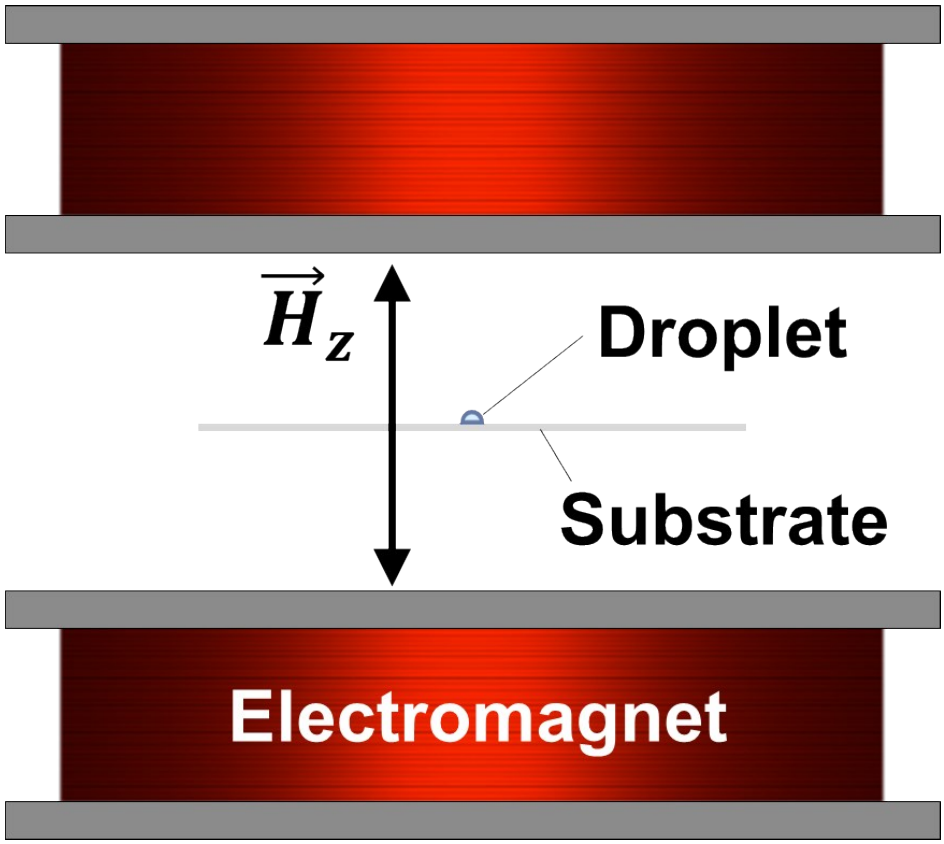

Figure S1. A scaled view of the experimental setup. The diameter of each electromagnetic coil is 130 mm. Two electromagnetic are separated by 70 mm. The diameter of a water droplet ranges from 2 to 4 mm. The fluctuation in the magnitude of the magnetic field is less than 1 Gauss around the droplet where the applied field amplitude is 35 Gauss in the system.

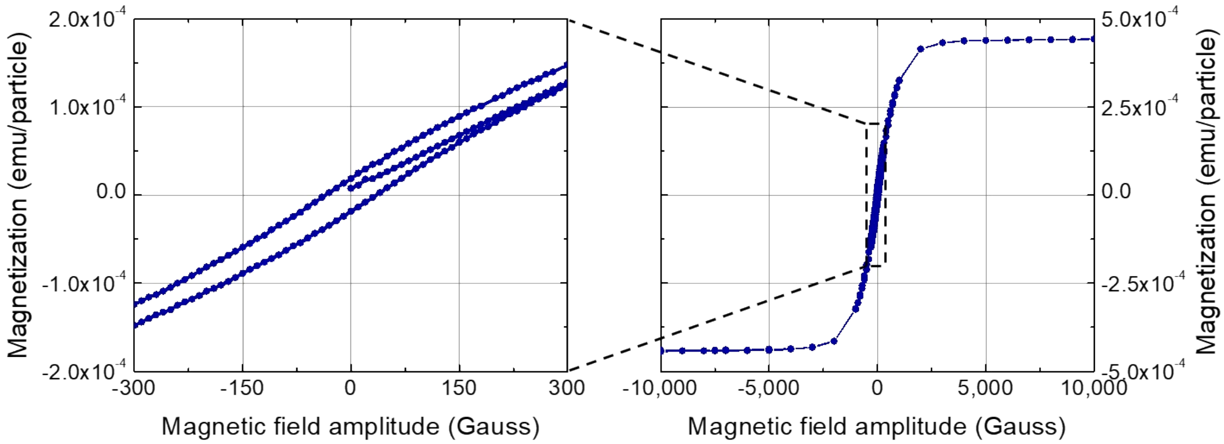

Figure S2. A magnetic hysteresis curve of ferromagnetic Ni particles measured by a SQUID. The measurement reveals that the magnetic moment at the 35 Gauss field (the amplitude used in our experiments) is 2×10^{-5} emu per particle and the saturated magnetic moment is 4.4×10^{-4} emu per particle.

The phenomenon of magnetic rolling in a uniaxial magnetic field relies on mechanical responsiveness of the ferromagnetic particles to the changes in the external magnetic field. The upper frequency of the external field oscillations is limited by a torque balance and results in $2\pi f_{max} \sim mH_0/(8\pi\eta R^3)$, where m, H_0, η, R are respectively the magnetic moment of the particle, the amplitude of the external magnetic field, dynamic viscosity of the liquid, and the radius of the particle. For the Ni particles and water used in the experiments $f_{max} \sim$ 1.2kHz. Above this characteristic frequency, a ferromagnetic particle does not exhibit any mechanical response. In addition, remnant magnetic moments of Ni particles rely on internal dynamics of the magnetic domain walls (pinned by defects) inside of each particle. When magnetic domain walls get de-pinned (due to increasing torque with the frequency of the external field) magnetic particles lose their "pinned" moment and reorientation of the magnetic moments proceeds without mechanical rotation of the particle. For Ni particles used in the experiments this frequency is close to 200Hz.

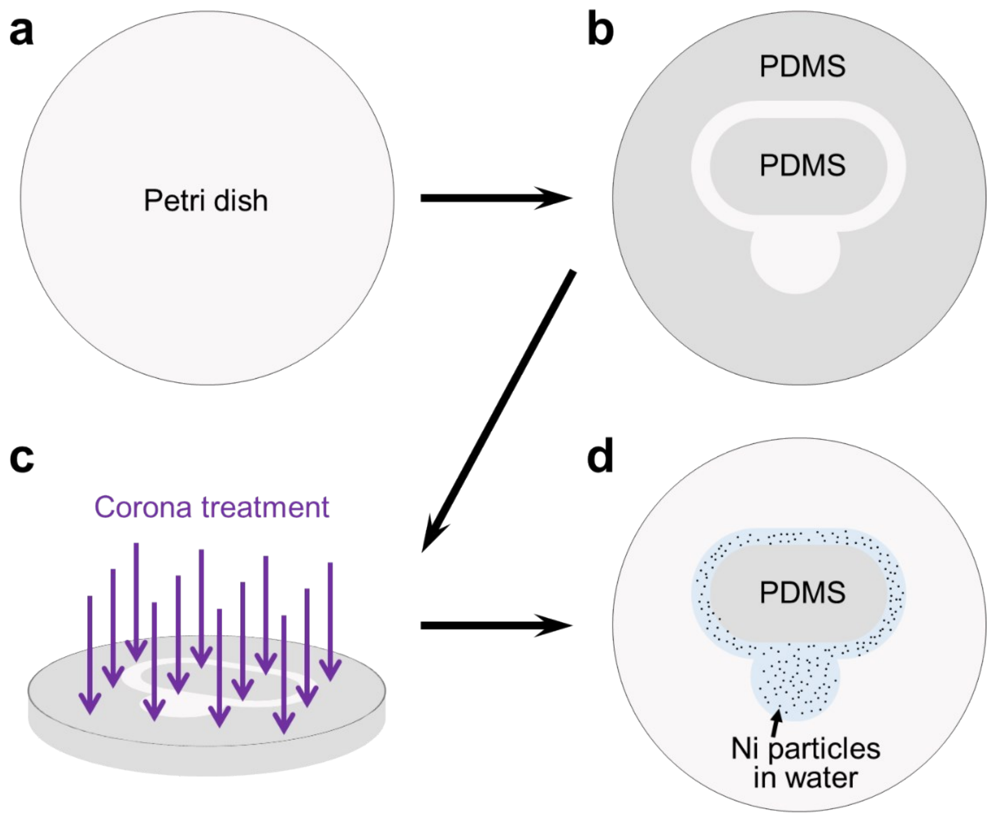

Figure S3. Schematic illustration of the fabrication process for a micro-pump device. (**a**) A bare Petri dish substrate. (**b**) A Petri dish masked with a patterned polydimethylsiloxane (PDMS). (**c**) Selective hydrophilization on the Petri dish by corona treatment through the patterned PDMS mask. (**d**) Selective wetting of a water suspension of Ni particles on the pre-defined hydrophilic pattern with a pump device design.

The design guidelines for the micro-pump:

The micro-pump architecture should include a circular chamber in the design that allows the rollers, acting as a fluid carrier, to continue circulating in the devices. The dimension of the chamber can be varied widely, however it is best to select the dimension of the micro-pump chamber in from about 10 to 100 particle sizes that is in the range of a characteristic length-scales of stable freestanding roller vortices, and ensures the efficient synchronization between the rollers, that in turn enables the switching of the chiral state of motion in the chamber in a repeatable manner.

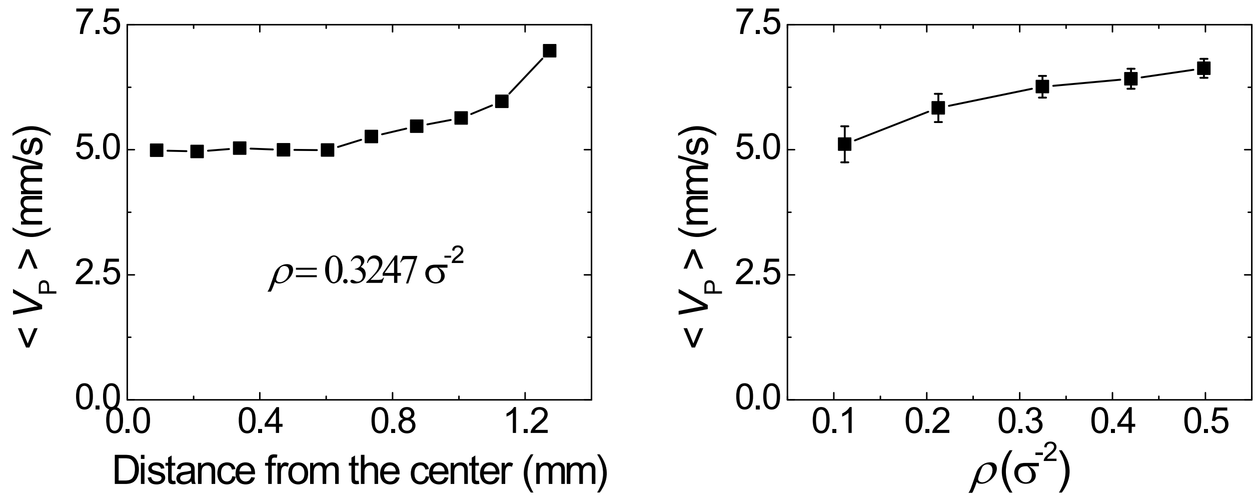

Figure S4. The mean roller velocity, $< V_P >$, as a function of (**left**) position and (**right**) density, ρ. (left) The magnetic rollers at the edge of the droplet exhibit higher $< V_P >$ because the presence of a confining elastic border along with the capillary forces at the droplet edge effectively reduces the rotational diffusion of the rollers and increases their persistence length. In comparison, the magnetic rollers at the droplet center exhibit relatively lower $< V_P >$ due to their lower persistence length. (right) $< V_P >$ increases with ρ as more rollers get close to and synchronized with the rollers at the droplet edge.